EVOLUTION OF THE MACHINE IMPEDANCE FOLLOWING THE ESRF UPGRADE TO LOW GAP NEG COATED ALUMINIUM CHAMBERS

T.F. Günzel, T. Perron, L. Farvacque, J.L. Revol, ESRF, Grenoble, France

Abstract

The installation of 5 meter-long, 8 mm vertical aperture insertion device (ID) aluminum chambers coated in house with non evaporable getter material (NEG) is progressing at a rate of one chamber per shutdown. The evolution of impedance with associated consequences on instability thresholds, following the installation of a number of low aperture insertion device chambers, will be reported. In particular, the impedance measurement using beam orbit bump method made it possible to identify and replace the chambers with the highest impedance. Correlation with the evolution of the instability thresholds and the theoretical prediction will be discussed. It was observed that change in vertical aperture has an important effect on the horizontal threshold.

INTRODUCTION

Over the past 2 years stainless steel (SS) chambers of different types: NEG-coated copper-covered stainless steel chambers (NEG/Cu/SS) of 8mm, pure SS of 11mm aperture and a SS-minigap of variable aperture, have been removed in favour of NEG-coated aluminium chambers (NEG/Al) with a vertical aperture of 8mm. This development was driven by the lower production costs and the acquired capability of the ESRF to carry out the NEG-coating in-house[1]. The measurement of effective impedance with the bump method showed that the NEG-coated aluminium chambers have less effective impedance than the NEG/Cu/SS-chambers (both of 8mm vertical aperture). Therefore, an improvement of the transverse impedance budget on both planes was expected. This paper reports on the observed increase of the single bunch thresholds at zero chromaticity effected by the vacuum chamber exchange. The numerical impedance model for the ESRF ring will be explained followed by the bump method for effective impedance measurement. Finally, the effect on the single bunch threshold in both planes as a result of the vacuum chamber evolution is discussed.

Impedance Model

The numerical impedance model[2] is based on numerical evaluation of the impedance of most vacuum chamber elements along the ring with the 3D-code GdfidL[3] and analytical calculation of the resistive wall impedance. As most ESRF-chambers can be considered as 2 parallel plates, the overall wake contains a component being quadrupolar in terms of the test particle and a component being dipolar in terms of the source particle. On the vertical plane both parts add up but on the horizontal plane the quadrupolar part has nearly the same absolute value as the dipolar part. Both therefore nearly cancel out due to their opposite signs. The effective impedance (see formula (1)) budgets of both planes based on the dipolar part has been established (fig. 1). The result shows that many different types of elements contribute to the vertical impedance budget whereas the low-gap chambers dominate in the horizontal impedance budget. The β-function distribution along the ring is responsible for that. Whereas the horizontal β-function assumes high values in the even-numbered low-gap sections and moderate values in the remaining part of the cells, the values of the vertical β-function are low in all straight sections and pretty high in the remaining part of the cell. The in-vacuum undulators are, in both budgets, not of primary importance because, apart from one, all are in odd-numbered cells with moderate horizontal and low vertical β-function. Furthermore they are 2.5 times shorter than standard low-gap chambers and are inside equipped with a CuNi-sheet providing good conductivity.

In order to reproduce the measured tune shifts, dipolar and quadrupolar components were distinguished and were processed separately[2]. The quadrupolar component is responsible for the incoherent tune shift, whereas the dipolar component produces the tune shifts of the coherent modes. Finally, the incoherent tune shift was added on all coherent modes in the same way. This leads to steeper slopes of the mode detuning in the vertical plane. In the horizontal plane, as the incoherent horizontal

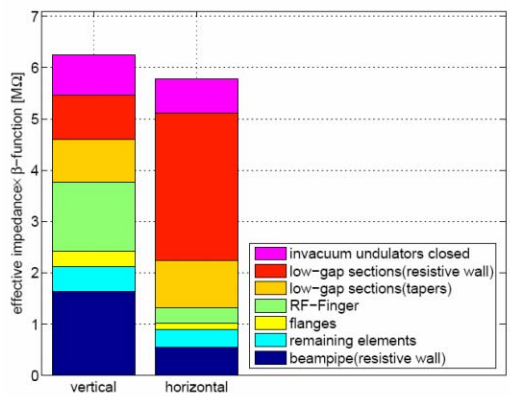

Figure 1: Effective vertical and horizontal impedance budget weighted by the local β-function based on numerical calculation (bunch length 5mm). It shows that the vertical impedance is distributed all along the machine whereas the horizontal impedance is dominated by the low-gap chambers.

tune shift is opposite to the vertical one, the coherent and incoherent tune shift nearly cancel out each other resulting in a (quasi)-constant total horizontal tune shift. The mode detuning and the instability thresholds were calculated assuming mode coupling[4] on the basis of the

developed model and compared to the measured modes. A current dependent bunch length was assumed. Therefore the calculated detuning curves had to be correctly normalized on the zero current synchroton frequency. This changes especially the slope of mode 0. The model predicted the threshold of 1.1mA vertically and of 1.2mA horizontally (fig.4 and fig.5).

The Local Bump Method

The local bump method was first introduced around the same time at BINP[5] and ALS[6] and implemented at the ESRF in 2002[7]. The principle of the method is to locally displace the beam from its axis by applying a closed bump of large amplitude, and to record the effect of impedance on the closed orbit.

Once the beam is displaced, its closed orbit will be affected by an impedance kick proportional to the beam displacement and the imaginary part of the effective impedance. If a subtraction is made between a test orbit recorded at high intensity per bunch and a reference orbit measured at zero current, only the distortion induced by the impedance kick is left. This distortion can be fitted by the response of the beam orbit to a kick at the location of the bump, resulting in the evaluation of the kick strength.

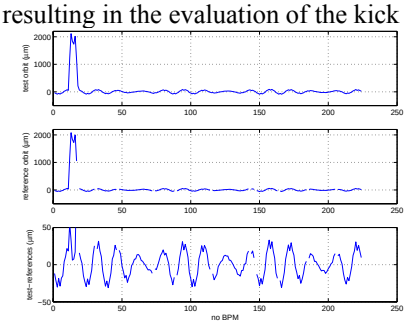

Figure 2: Measurement sequence: on top the test orbit (10mA single bunch), in the middle the reference orbit (10mA 992 bunch), on bottom the difference between both shows the distortion due to the impedance kick.

Assuming a gaussian distribution for the bunch, the kick angle is related to the effective impedance by:

$$\theta_{Kick} = \frac{I \times z_{Bump}}{2\sqrt{\pi} \times f_0 \times \sigma_t \times \left(E/e\right)} \times \Im\left(Z_{\perp eff}\right)$$

Where θ is the kick angle, z is the bump amplitude, f_0 the revolution frequency, I the bunch current and σ_t the RMS bunch length in seconds.

The effective impedance is defined by the formula:

$$Zeff = \frac{\sum_{\omega} Z_{(\omega)} \times \left|\sigma_{\omega}\right|^2}{\sum_{\omega} \left|\sigma_{\omega}\right|^2} \qquad (1)$$

were $Z_{(\omega)}$ is the impedance and $\sigma_{(\omega)}$ is the longitudinal amplitude spectrum of the beam.

Once the strength of this kick is recorded, one can deduce the imaginary part of the effective impedance of the section where the bump is applied. It is of great interest as impedance effects can be measured locally, allowing the comparison of different elements. The main motivation behind this was to be able to follow up the evolution of machine impedance while straight section vacuum chambers where exchanged.

Since in this method the source and the test particle have the same offset, the measured effective impedance contains both dipolar and quadrupolar parts. Therefore, if both parts are assimilated to pure dipolar impedance it leads to an overestimation of the effective impedance. On the other hand, as horizontal and quadrupolar part cancel out in the horizontal plane the bump method cannot be applied on the horizontal plane. However, if in the parallel plate approximation dipolar impedance should represent about 2/3 of the overall result in the vertical plane. The remaining 1/3 is the quadrupolar part, whose value on the horizontal plane is the same but of different polarity (sign). As in the horizontal plane the value of horizontal dipolar impedance and of the quadrupolar part are nearly the same apart from the sign, the quadrupolar part can be considered effectively as an estimate for the value of the horizontal impedance.

The local bump method was used to characterise different chamber types. The result is illustrated in fig.3. It shows clearly that NEG/Al-chambers have less effective impedance than NEG/Cu/SS-chambers. Furthermore, the effective impedance value of the different SS-chambers varies significantly whereas the impedance value of the NEG/Al-chamber is more reproducible. In the impedance model the wall of the NEG-coated chambers was assumed to consist of 2 layers (NEG on Al) or (NEG on Cu) according to [8]. This modelisation was not sufficient to explain the measured difference between the impedance of NEG/Cu/SS-chambers of 8mm aperture and that of NEG-coated Al-chambers of the same aperture. Possible explanations are different surface roughness (which was not taken into account), uncertainty of the conductivity of the NEG-coating, discontinuity of the copper layer and fabrication errors of the NEG/Cu/SS-chambers which can lead to significant deviations from the geometry used in the simulation.

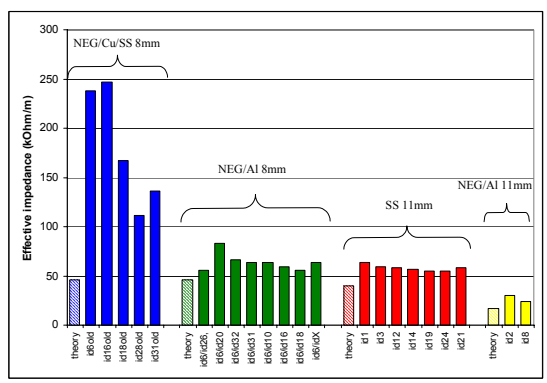

Figure 3: Comparison of different low-gap chamber types calculated values displayed as hatched bars are about 30% smaller than the measured ones (except for NEG/Cu/SS chambers where it is more)

Evolution of Low-Gap Chamber Installation

The mode detuning and the single bunch instability thresholds were observed at different moments of the low-gap chamber installation in the ESRF-ring (table 1).

chamber type	sept ' 03 measurement of horizontal detuning	june '04 measurement of vertical detuning	feb.'05 Re-measurement of horizontal + vertical detuning
5m long 8mm Al/NEG	3	6	9
In vacuum undulators 2m long	4	7	7
5m long 8mm NEG/Cu/SS	4	3	1
5m long 11mm SS	11	8	8
1.2m long minigap SS	1	1	0
2m long 15mm SS	1	0	0
3.3m long 11mm SS	1	1	0

Table 1: The quantity of low-gap vacuum chambers when the mode detuning was measured.

We will report on the variations of detuning at nearly zero chromaticity in single bunch which occur in the intervals defined in the table. Particular attention is drawn to the replacement of the NEG/Cu/SS-chambers of 8mm aperture in ID16 and ID18 which had been identified as having the largest impedance by two NEG/Al-chambers of 8mm aperture between June '04 and Februray '05. Before this replacement the variation of the vertical threshold had been, in the most cases, minor. However, the measurements before and after the replacements

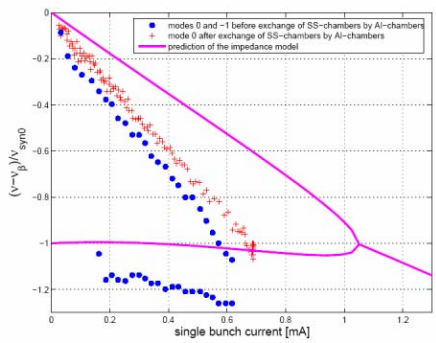

Figure 4: Measured and calculated vertical mode detuning versus single bunch current. Threshold changes from 0.65mA to 0.71mA. ν_{SYN0} is the zero current synchrotron tune. The bunch length was assumed current-dependent.

showed a sensible change. The vertical threshold raised from 0.65mA to 0.71mA (fig.4). Nevertheless due to the low β-function in the cells ID16 and ID18, the vertical impedance reduction was only moderate. The calculated simulation of evolution of low–gap chamber installation was so small that no variation is visible.

Initially measured to be at 1.3mA the horizontal threshold was remeasured directly after the exchange of chamber in ID16 (1.7mA) and again after the exchange of chamber in ID18 (2.7mA). The model only predicts a change of 1.1mA to 1.2mA in threshold (fig.5). This is due to a lack of the impedance model to correctly simulate the large impedance of the NEG/Cu/SS-chambers. However, by taking the impedance change measured by the bump method, assimilating 1/3 of the value to horizontal impedance (as explained in the previous section) and multiplying it by the local horizontal β-function of 35m, a change of 3.54MΩ is obtained which can qualitatively explain the strong increase of the horizontal threshold. Nevertheless the enormous raise and the nature of the horizontal threshold have still to be better understood.

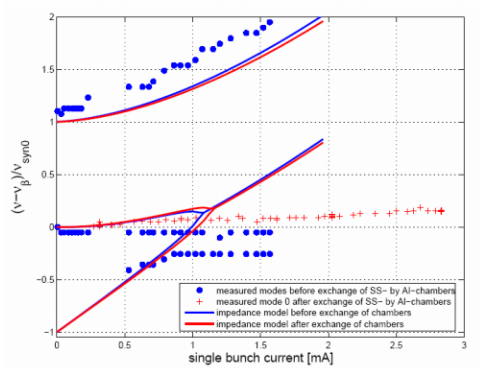

Figure 5: Measured and calculated horizontal mode detuning, threshold changes from (blue) 1.3mA (calculated 1.1mA) to (red) 2.7mA (calculated 1.2mA). The slope of mode 0 increases due to the current-dependent bunch length.

CONCLUSION

The bump method made it possible to identify the low-gap chambers with the largest impedance in the ESRF-ring and to replace them with NEG-coated Al-chambers with significantly less impedance. The numerical impedance model allowed to interpret the observed changes of the single bunch thresholds at zero chromaticity, in particular on the horizontal plane. The impedance model can still be improved by a better repartition of impedance on both planes. Furthermore the dynamics on the horizontal plane being more complex than expected merits further studies. The observed horizontal effect induced by vertical low-gap chambers has important consequences on the design of future synchrotron light sources.

REFERENCES

[1] M. Hahn, R. Kersevan, Status of the NEG-coating at the ESRF, this conference (PAC 2005)
[2] T.F.Günzel, Coherent and incoherent tune shifts deduced from impedance modelling in the ESRF-ring, EPAC 2004
[3] W. Bruns, GdfidL, www.gdfidl.de
[4] Y.H.Chin, MOSES, CERN/LEP-TH/88-5
[5] V.A. Kiselev, V. Smaluk, V.Zorin, Transverse Coupling Impedance of the VEPP-4M Collider: Measurements and Simulations, PAC 2001
[6] L. Emery, G. Decker, J. Galayada, Local bump method for measurements of transverse impedance of narrow-gap ID chambers in storage rings, PAC 2001
[7] T. Perron, L. Farvacque, E. Plouviez, Vertical effective impedance mapping of the ESRF storage ring, EPAC 2004
[8] A.Burov, V.Lebedev, Transverse resistive wall impe-dance of a multi-layer round chamber, EPAC 2002